Synthesis and characterization of photosensitive TiO₂ nanorods by controlled precipitation route

**D. P. Dubal · D. S. Dhawale · A. M. More ·
C. D. Lokhande**

Abstract Nanocrystalline TiO₂ thin films have been successfully synthesized by controlled precipitation route. These films are further annealed at 623 K for 2 h. The change in structural, morphological, optical, and wettability properties are studied by means of X-ray diffraction (XRD), Fourier transform infrared spectrum (FTIR), scanning electron microscopy (SEM), optical absorption, and contact angle measurement. From the XRD pattern it is clear that the as-grown TiO₂ films are amorphous in nature which becomes polycrystalline after annealing. The FTIR study reveals the formation of TiO₂ compound. Scanning electron micrographs shows that the as-grown TiO₂ film consists of agglomerated nanograins well covered to the substrate surface which gets converted into vertical nanorods after annealing. As-deposited and annealed TiO₂ films showed hydrophilic behavior as water contact angles were 24° and 32°, respectively. The optical absorption study reveals the small red shift due to annealing and attributed to grain size. The annealed TiO₂ film showed conversion efficiency of 0.037% in photoelectrochemical cell with 1 M NaOH electrolyte.

Introduction

Nanometer-sized materials have recently gained a considerable amount of attention of their unique physical and chemical properties, because of their large surface to volume ratio and quantum size effect. The physical and chemical properties of nano TiO₂ are dependent on the size, morphology, and crystal structure. TiO₂ nanomaterials, such as nanoparticles, nanotubes, nanorods, etc., have attracted a great deal of interest because of their unique optical, electronic, and optoelectronic properties and promising applications in solar energy conversion, photocatalysis, sensing, optoelectronic devices, and photochromic devices [1–5]. It is well known that one-dimensional architectures such as nanorods, nanowires, and nanotubes play prominent roles in functional devices due to their dimensionality and quantum confinement phenomena. The physicochemical properties of TiO₂ nanomaterials vary in their size and morphology. TiO₂ has three distinct crystalline phases in nature: brookite, rutile, and anatase, where rutile is the most stable phase and possesses field emission property, and anatase has been widely used in dye-sensitized solar cells and photodegradation due to its high photoactivity.

Zhu et al. [6] found that phase transitions from the titanate nanostructures prepared from TiOSO₄ to TiO₂ polymorphs took place readily in wet-chemical processes at temperatures close to ambient. Yu et al. [7] synthesized single-crystalline anatase nanorods via hydrothermal transformation of H-titanate fibers prepared by an alkaline hydrothermal reaction at 200°C. Nian et al. [8] studied the hydrothermal treatment of sodium titanate nanotube suspensions at a pH range from 2.2 to 6.9, and anatase nanorods with an aspect ratio up to 6 and a long axis along the anatase (001) were obtained at a pH slightly less than 7. Wong et al. [9] presented a size- and shape-dependent morphological transformation during the hydrothermal soft chemical transformation of H-titanate nanostructures into their anatase titania counterparts in neutral solution. Performance of TiO₂ for technical applications is strongly influenced by its morphology, crystallite size, crystalline

D. P. Dubal (✉) · D. S. Dhawale · A. M. More ·
C. D. Lokhande
Department of Physics, Thin Film Physics Laboratory,
Shivaji University, Kolhapur 416004, Maharashtra, India
e-mail: dubal_deepak@yahoo.co.in

phase, and impurity type concentration. Porous nanocrystalline TiO_2 have attracted a great interest because; the function and performance of the material are strongly dependent on its morphology. Porosity leads to a comparatively large internal surface area, which are advantageous for many applications where a good accessibility to the film surface becomes necessary. Porous materials as electrode material exhibit good electrochemical performance because these materials possess both a high surface area and pores which are adapted to the size of ions. Accordingly, the advance of synthetic methods, in which the crystalline phase, size, and shape of the TiO_2 nanocrystals can be controlled, is of importance. In recent years, many studies related to the synthesis of anatase TiO_2 have been focused on the control of morphology as well as particle size.

TiO_2 thin films have been prepared by many growth techniques, such as RF-metal–organic chemical vapor deposition (MOCVD) [10], sol–gel process [11], electrodepositon [12], and chemical bath deposition (CBD) method [13]. As compared to the other deposition methods, controlled precipitation route is an attractive one because of its own advantages such as simplicity, reproducibility, non-hazardous, cost effectiveness, etc. It is well suited for producing large-area thin films at low temperature and hence avoids oxidation or corrosion of metallic substrate [14].

In the present work, we demonstrate the formation of controlled TiO_2 nanorods, on indium–tin-oxide (ITO) coated glass substrates in a template-free controlled precipitation route. The TiO_2 nanorods are found to be well aligned and perpendicular to the ITO substrate. X-ray diffraction, Fourier transforms infrared spectroscopy, and scanning electron microscopy techniques are used to elucidate crystal structure, chemical bonding, and surface morphology. In addition, extensive photosensitive studies of these TiO_2 nanorods have been performed.

Experimental

An aqueous solution composed of titanium trichloride, hydrogen peroxide was first prepared. In brief, 0.1 M $TiCl_3$, 15% HCl was added dropwise to a well-stirred hydrogen peroxide (H_2O_2, Molychem, 30 wt%) and water solution. The pH was adjusted between 2.0 and 3.0 using a mixture of 30% liquid ammonium hydroxide with constant stirring. A transparent solution with a reddish-yellow color was obtained after vigorous stirring for 30 min at room temperature. Glass and ITO coated glass substrates were washed with chromic acid and in an ultrasonic bath at room temperature for 30 min. These cleaned substrates were immersed in the above bath and the bath was heated. When the bath attains the temperature of 343 K, the precipitation was started in the bath. During the precipitation,

heterogeneous reaction occurs on the substrate and deposition of TiO_2 took place on the substrate. The TiO_2 films were annealed in air at 623 K for 2 h and used for further characterizations.
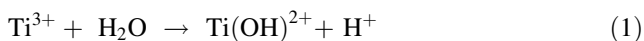
The thickness of the TiO_2 film was measured by weight difference method using sensitive microbalance. The crystallinity of as-grown and annealed TiO_2 films was analyzed with Philips X-ray diffractometer (Philips PW 3710) with Cr K_α radiation ($\lambda = 2.2896$ Å). The Fourier transform infrared (FTIR) spectrum of the sample was collected using Perkin Elmer, FTIR Spectrum one' unit. Detailed surface images were obtained by means of field emission scanning electron microscope observation on a (FE-SEM, Model: JSM-6160) electron microscope. The optical absorption studies were carried out within the wavelength range 350–850 nm for as-grown and annealed TiO_2 films using Systronics spectrophotometer-119, with glass substrate as reference. In order to study interaction between liquid and thin film surface, contact angle measurement was carried out by Rame-hart, USA equipment with CCD camera. The photoelectrochemical properties of films were investigated using the 263A EG&G Princeton Applied Research Potentiostat forming a three-electrode system comprising TiO_2 film as working electrode, graphite as counter electrode and SCE as reference electrode in 1 M NaOH.

Results and discussion

Film formation and reaction mechanism

In controlled precipitation method, reaction takes place between the dissolve precursors generally in aqueous solution at low temperature. When the solution is saturated, the ionic product of anion and cation is equal to solubility product of metal chalcogenide/oxide and when it exceeds, precipitation occurs and ions combine on the substrate and in the solution to form nuclei. Generally metal ions are complexed and chalcogenide ions are chosen in such a way that reaction take place between slowly released metal ions to form product in powder or thin film form. Depending upon the optimized preparative conditions such as bath temperature, pH of resultant solution, deposition temperature, solution concentration, the film growth can takes place by ion-by-ion condensation on the substrate.

In present investigation, titanium (III) chloride is first hydrolyzed by H_2O in a mixture solution of H_2O and H_2O_2, which then immediately reacted with H_2O_2 to form a peroxotitanate solution. It was found that the initial pH, just after addition of H_2O and H_2O_2 to the titanium (III) trichloride solution, was ~ 1.00; this increased to ~ 3 after complete digestion of hydrolyzed titanium hydroxides. The reaction mechanism is as follows

$$Ti^{3+} + H_2O \rightarrow Ti(OH)^{2+} + H^+ \qquad (1)$$

$$2H_2O_2 \rightarrow 2H_2O + O_2 \qquad (2)$$

The resulting peroxotitanate solution further dissociates with increase in pH of the solution to form TiO_2 solid film onto the substrate.

$$Ti(OH)^{2+} + O_2 \rightarrow TiO_2 + 2OH^- \qquad (3)$$

Thus, the uniform and well-adherent TiO_2 films are deposited on the glass substrate.

Thickness measurement

The thickness of the TiO_2 film was measured by a gravimetric weight difference method in terms of the weight of TiO_2 deposited on the glass substrate per unit area (mg/cm^2), since the accurate measurement of TiO_2 film thickness was not possible due to the rough morphology and porosity of the film [15]. Figure 1 shows the film thickness variation of TiO_2 thin film with deposition time. The rate of increase in the thickness is nonlinear, which has been attributed to the growth by nucleation and coalescence process. More nucleation sites contribute to coagulation during the growing procedure. Furthermore, slight decrease in film thickness observed could be attributed to the formation of outer porous layer and/or the film which may develop stress to cause delamination, resulting in peeling off the film after the film reaches at maximum thickness. The terminated thickness at which the highest amount of TiO_2 deposited on the substrate was 1.29 μm.

Structural study

Figure 2a and b shows typical X-ray diffraction patterns of as-deposited and annealed TiO_2 thin films on glass substrate, respectively. It is evident from XRD patterns that TiO_2 thin films are polycrystalline and has rutile phase.
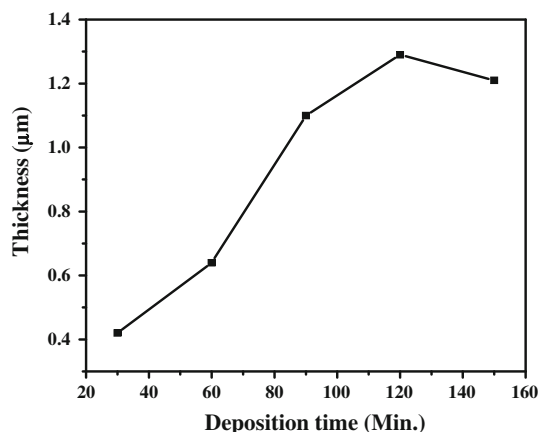

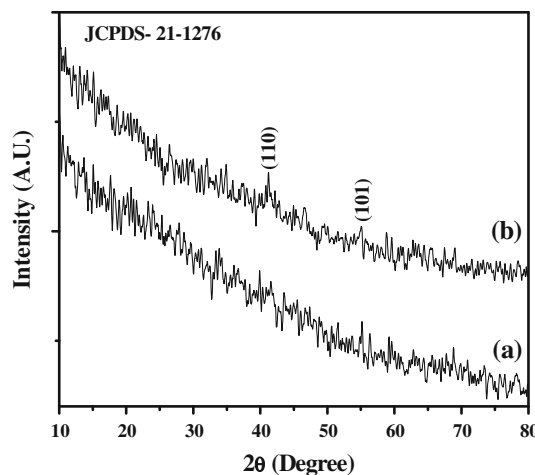Fig. 1 Variation of TiO_2 film thickness with deposition time

Fig. 2 XRD patterns of (a) as-deposited and (b) annealed TiO_2 thin films

The XRD pattern indicates the presence of (110), and (101) planes of TiO_2 material which is in good agreement with JCPDS cards no. 21-1276. The XRD pattern of as-deposited films probably means that the film consisted of hydrous TiO_2 colloidal particles with low crystallinity. Intensity of (110) and (101) peaks is increased as an effect of annealing, which attributed to the improvement in crystallinity. The grain size was estimated using Scherrer's formula

$$D = \frac{0.9\lambda}{\beta \cos \theta} \qquad (4)$$

where, β is the broadening of diffraction line measured at half maximum intensity (radians) and $\lambda = 2.2897$ Å is the wavelength of the Cr K_α X-ray. The grain size was found to be 56 nm for (110) plane.

FTIR study

Figure 3 shows FTIR spectra of the (a) as-deposited and (b) annealed TiO_2 samples within the wavelength range 400–4000 cm^{-1}. The absorption at 3409 cm^{-1} indicates the presence of hydroxide group [16]. The absorption peak around at 1634 cm^{-1} may be due to the bending vibration of hydroxyl groups of molecular water [17]. The absorption peak at around 1000 cm^{-1} is assigned to characteristic stretching vibration of peroxo groups. The strong absorption peak around at 649 cm^{-1} is associated with the characteristic vibrational mode of anatase TiO_2 [18]. As-deposited TiO_2 showed the higher depth at 3409 cm^{-1} than annealed one, which attributed to removal of hydroxide after heat treatment. Hence, results indicate the presence of Ti–O bond, peroxo groups, and –OH groups for as-deposited film, whereas after annealing the peaks attributed to the peroxo groups and –OH groups were almost disappeared. Less
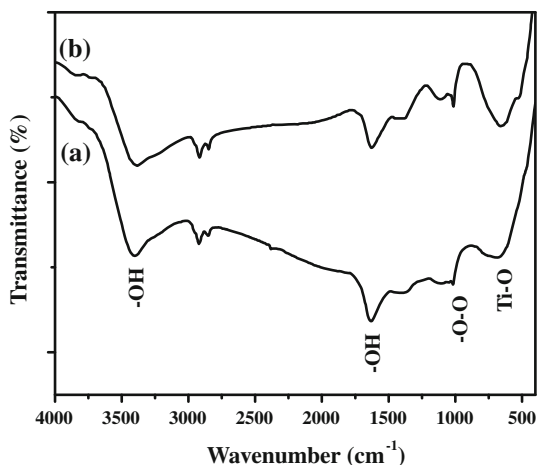
Fig. 3 FTIR spectra of (*a*) as-deposited and (*b*) annealed TiO$_2$ samples

intense hydroxide and hydroxyl groups from water found in the annealed TiO$_2$ may be due to the fact that the spectrum was not recorded in situ and some readsorption of water from the ambient atmosphere might have occurred.

Surface morphological study

Figure 4a and b shows the field emission scanning electron micrographs (FE-SEM) of as-deposited and annealed TiO$_2$ thin films at 50,000× magnification, respectively. From micrograph (Fig. 4a) it is seen that the deposits consists of well defined agglomerated multigrain structure having irregular shapes and sizes due to the low temperature deposition method. The approximate size of this multigrain structure is about 140 nm. Some pores and overgrowth is also seen in the micrographs. Mane et al. [19] prepared TiO$_2$ by CBD method and reported the formation of spherical, compact, and randomly oriented grains. After annealing this multigrain structure completely gets converted into well-defined conical nanorods. The approximate length and diameter of these nanorods is ~110 and 25 nm, respectively (Fig. 4b). The barrier effect of intercrystalline TiO$_2$ is greatly decreased by using long nanorods instead of a porous TiO$_2$ thin film composed of accumulated nanosized particles. This might contribute to the easier electron transfer and decrease the Ohmic loss through the TiO$_2$ layer in dye-sensitized solar cells [20].

Optical studies

Figure 5a and b shows optical absorption spectra for as-deposited and annealed TiO$_2$ thin films within 350–850 nm wavelength range. The absorption edge was found to be 450 nm as seen from inset of Fig. 5. These spectra reveal that TiO$_2$ film has low absorbance in the visible region,
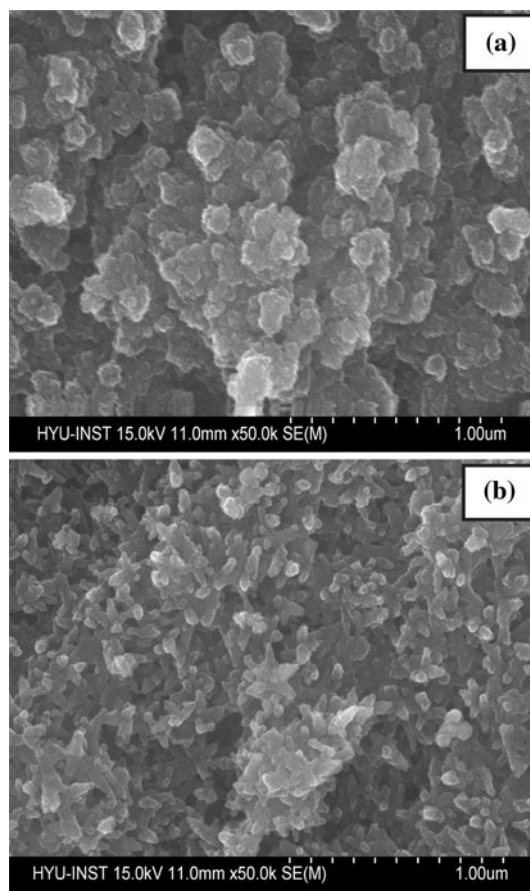

Fig. 4 Scanning electron micrographs of **a** as-deposited and **b** annealed TiO$_2$ thin films at ×50,000 magnification
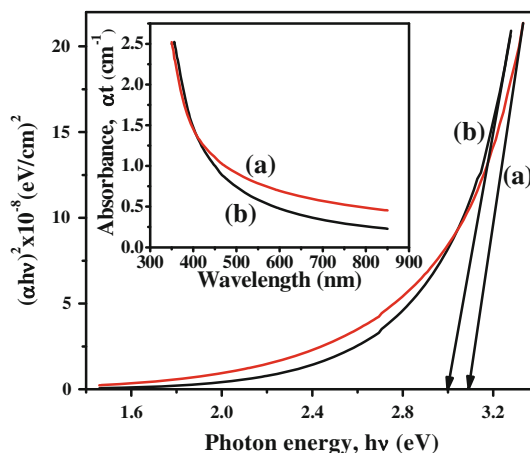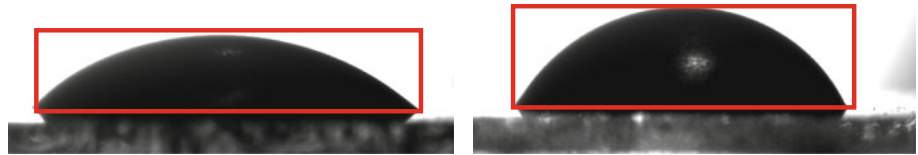

Fig. 5 Plot of $(\alpha h\nu)^2$ vs. photon energy hν of (*a*) as-deposited and (*b*) annealed TiO$_2$ (*inset* shows variation of absorption (αt) with wavelength (λ) of (*a*) as-deposited and (*b*) annealed TiO$_2$ on glass substrate)

which is a characteristic of TiO$_2$. The optical band gap (E_g) for as-deposited and annealed TiO$_2$ film is calculated on the basis of optical absorption using the following equation,

$$\alpha = \frac{A(E_g - h\nu)^n}{h\nu}$$

where $h\nu$ is the photon energy, and A is constant. The exponent 'n' depends upon the type of transition and has values of 1/2 and 2 for direct and indirect transitions, respectively. By plotting the graph of $(\alpha h\nu)^2$ versus $h\nu$ (Fig. 5), it becomes possible to determine the nature of transition involved. The extrapolation of straight line portions of the plot ($h\nu$ greater than E_g) to the zero absorption coefficient gives measurement of energy gap. Both plots show a linear dependence at $h\nu$ greater than E_g, therefore extrapolation of the straight line portions of the curves to the zero absorption coefficient gives band gap of 3.1 and 3.0 eV for as-deposited and annealed TiO_2 films, respectively. Due to the improved grain size of annealed, the absorption edge showed red-shift up to some extent. The widened band gap of the TiO_2 films is attributed to the contribution of quantum size effect [21].

Wettability test

Controlling and/or modifying the surface wettability are important, which involves the interaction between a liquid and a solid in contact. Measurement of surface water contact angle is inversely proportional to the wettability and can be determined by Young's relation [22]. Figure 6 shows the water contact measurements for (a) as-deposited, and (b) annealed TiO_2 thin films. Interestingly, as-deposited TiO_2 exhibits hydrophilic behavior (24°), as water contact angle is less than 90°. The shape of water droplet on the film is shown in Fig. 6a. Further, for annealed films, the water contact angle slightly increases to 32°. The droplet shape on the surface of annealed TiO_2 film was more spherical (Fig. 6b). Increase in water contact angle after annealing attributed to (a) non-spherical nature of the grains and (b) topographical change in structure. Due to the conversion from spherical nanograins to nanorods after annealing prevents the water from adhering to the film results into increase in water contact angle. Similar type of result has been reported by More et al. [23].

Photovoltaic response

A photoelectrochemical cell (PEC) is based on the junction between semiconductor and an electrolyte. The current–voltage (I–V) characteristic of a typical ITO/TiO_2/1 M
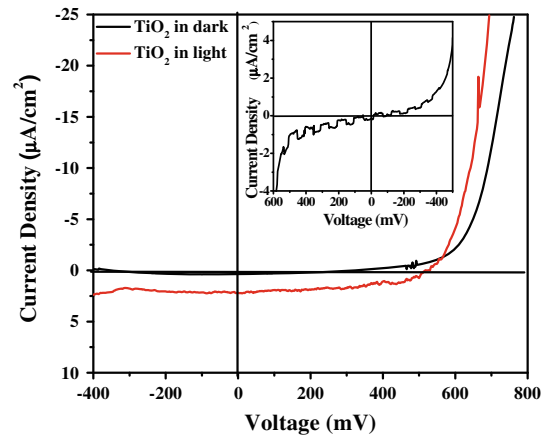

Fig. 7 I–V characteristics of annealed TiO_2 film under illumination of white light (50 mW/cm^2). *Inset* shows the I–V characteristic under chopped light

NaOH/graphite cell in the dark and under illumination (50 mW/cm^2) is shown in Fig. 7. In the dark, the nonlinear nature of I–V curve predicts that the TiO_2 makes rectification contact with the electrolyte. Inset of Fig. 7 shows the photosensitivity under chopped light conditions carried out to study the response of the TiO_2 films. The photocurrent is obtained in the order of $\mu A/cm^2$. The photoconversion efficiency 0.037% with fill factors 0.44 and flat band potential -400 mV/SCE were observed. In present investigation, low efficiency is attributed to less absorption of visible light in TiO_2 due to its wide band gap.

Conclusion

Here, we have successfully synthesized TiO_2 nanorods by simple and inexpensive controlled precipitation route and further used for photoelectrochemical application. XRD pattern reveals that TiO_2 thin films are polycrystalline and has rutile phase. The TiO_2 compound formation was confirmed from FTIR study. Scanning electron micrographs reveals that the multigrain structure of as-deposited TiO_2 thin films completely gets converted into well-defined conical nanorods due to annealing. The optical absorption study reveals the small red shift due to annealing and attributed to grain size. Both the as-grown and annealed TiO_2 thin films are hydrophilic in nature as water contact angle is less than 90°. The strong influence of this electrode in spite of its wide band gap and substrate resistance on

photoelectrochemical performance with fill factor (0.44) and device conversion efficiency (0.037%) can motivate to check its feasibility in DSSC's devices.

References

1. Fujishima A, Honda K (1972) Nature 238:37
2. Chen X, Mao SS (2007) Chem Rev 107:2891
3. Bavykin DV, Friedrich JM, Walsh FC (2006) Adv Mater 18:2807
4. Yeredla RR, Xu H (2008) Nanotechnology 19:055706
5. Wang G, Wang Q, Lu W, Li J (2006) J Phys Chem B 110:22029
6. Zhu HY, Lan Y, Gao XP, Ringer SP, Zheng ZF, Song DY, Zhao JC (2005) J Am Chem Soc 127:6730
7. Yu Y, Xu D (2007) Appl Catal B Environ 73:166
8. Nian JN, Teng H (2006) J Phys Chem B 110:4193
9. Mao Y, Wong SS (2006) J Am Chem Soc 128:8217
10. Anpo M, Takeuchi M (2003) J Catal 216:505
11. Espinosa R, Zumeta I, Santana JL, Marinez-Luzardo F, Gonzalez B, Docteur S, Vigil E (2005) Solar Eng Mater Solid Cells 85:359
12. Lokhande CD, Min S-K, Jung K-D, Joo O-S (2004) J Mater Sci 39:6607. doi:10.1023/B:JMSC.0000044903.93296.a4
13. Lokhande CD, Lee E-H, Jung K-D, Joo O-S (2004) J Mater Sci Lett 39:2915
14. Mane RS, Lokhande CD (2000) Mater Chem Phys 65:1
15. Park BO, Lokhande CD, Park HS, Jung KD, Joo OS (2004) Mater Chem Phys 87:59
16. Karuppuchamy S, Jeong JM (2006) J Oleo Sci 55:263
17. Wang Y, Herron N (1991) J Phys Chem 95:525
18. Josea AN, Juan JT, Pablo D, Javier RP, Diana R, Marta IL (1999) Appl Catal A 178:191
19. Mane RS, Hwang YH, Lokhande CD, Sartale SD, Han S-H (2005) Appl Surf Sci 246:271
20. Jiu J, Isoda S, Wang F, Adachi M (2006) J Phys Chem B 110:2087
21. Monticone S, Tufeu R, Kanaev AV, Scolan E, Sanchez C (2000) Appl Surf Sci 162:565
22. Lokhande CD, Barkschat A, Tributsch H (2003) Sol Energy Mater Sol Cells 79:293
23. More AM, Gujar TP, Gunjakar JL, Lokhande CD, Joo O-S (2008) Appl Surf Sci 255:2682